WUB 03-03
ITP-BUDAPEST 593
DESY 03-022

WUB 03-03
ITP-BUDAPEST 593
DESY 03-022
hep-ph/0303080

arXiv:hep-ph/0303080 v1 10 Mar 2003

Electroweak instantons as a solution to the ultrahigh energy cosmic ray puzzle

Z. Fodor[a,b], S. D. Katz[c]*, A. Ringwald[c], and H. Tu[c]

[a] *Department of Physics, University of Wuppertal, Germany*
[b] *Institute for Theoretical Physics, Eötvös University, Budapest, Hungary*
[c] *Deutsches Elektronen-Synchrotron DESY, Hamburg, Germany*

Abstract

We propose a scenario in which a simple power-like primary spectrum for protons with sources at cosmological distances leads to a quantitative description of all the details of the observed cosmic ray spectrum for energies from 10^{17} eV to 10^{21} eV. As usual, the ultrahigh energy protons with energies above $E_{\rm GZK} \approx 4 \cdot 10^{19}$ eV loose a large fraction of their energies by the photoproduction of pions on the cosmic microwave background, which finally decay mainly into neutrinos. In our scenario, these so-called cosmogenic neutrinos interact with nucleons in the atmosphere through Standard Model electroweak instanton-induced processes and produce air showers which are hardly distinguishable from ordinary hadron-initiated air showers. In this way, they give rise to a second contribution to the observed cosmic ray spectrum – in addition to the one from above mentioned protons – which reaches beyond $E_{\rm GZK}$. Since the whole observed spectrum is uniquely determined by a single primary injection spectrum, no fine tuning is needed to fix the ratio of the spectra below and above $E_{\rm GZK}$. The statistical analysis shows an excellent goodness of this scenario. Possible tests of it range from observations at cosmic ray facilities and neutrino telescopes to searches for QCD instanton-induced processes at HERA.

*On leave from Institute for Theoretical Physics, Eötvös University, Budapest, Hungary.

1 Introduction

The puzzle of ultrahigh energy cosmic rays (UHECRs) is about 40 years old. About twenty mysterious events were observed above 10^{20} eV by five different air shower observatories (AGASA [1], Fly's Eye [2], Haverah Park [3], HiRes [4], and Yakutsk [5]; for reviews, see Ref. [6]). Though some small-angle clustering in the arrival direction of the UHECRs is observed, the overall event distribution is isotropic. This indicates that they originate from several sources. No source is known, however, within a distance of 50 Mpc. This is rather peculiar, since 50 Mpc is the characteristic distance ultrahigh energy nucleons travel before they loose a large fraction of their energy. A sharp drop around the Greisen-Zatsepin-Kuzmin (GZK) cutoff $E_{\rm GZK}\approx 4\cdot 10^{19}$ eV is therefore predicted in the cosmic ray spectrum [7]. The available data show no such drop[1].

The reason for the expected drop is a well established elementary process. Above $E_{\rm GZK}$, protons produce pions through the interaction with photons from the 2.7 K cosmic microwave background (CMB). The produced pions decay, resulting in the so-called cosmogenic neutrinos [9]. The attenuation length of protons above the GZK cutoff is about 50 Mpc. The basic question is: if the sources of ultrahigh energy cosmic rays are indeed at cosmological distances, how could they reach us with energies above 10^{20} eV? No conventional explanation is known for this question.

At the relevant energies among the known particles only neutrinos can propagate without significant energy loss from cosmological distances to us. It is this fact which led, on the one hand, to scenarios invoking hypothetical – beyond the Standard Model – strong interactions of ultrahigh energy cosmic neutrinos [9] and, on the other hand, to the Z-burst scenario [10, 11, 12].

In the latter, ultrahigh energy cosmic neutrinos (UHECνs) produce Z-bosons through annihilation with the relic neutrino background from the big bang. On earth, we observe the air showers initiated by the protons and photons from the hadronic decays of these Z-bosons. Though the required ultrahigh energy cosmic neutrino flux is smaller than present upper bounds, it is not easy to conceive a production mechanism yielding a sufficiently large one. In the near future, the neutrino telescopes AMANDA [13] and RICE [14], as well as the Pierre Auger Observatory [15] for extensive air showers, can directly confirm or exclude this scenario.

Scenarios based on strongly interacting neutrinos use the fact that the observed cosmic ray flux above $E_{\rm GZK}$ can be fairly well described by the predicted [16, 17] cosmogenic neutrino flux. In these scenarios, neutrinos with energies above $\approx 10^{20}$ eV originating from the GZK process are assumed to have a large cross-section for the scattering off nucleons and to initiate extensive air showers high up in the atmosphere, like hadrons. This is usually ensured by new types of TeV-scale interactions beyond the Standard Model, such as arising through gluonic bound state leptons [18], TeV-scale grand unification with leptoquarks [19], or Kaluza-Klein modes from extra compactified dimensions [20] (see, however, Ref. [21]); for earlier and further proposals, see Refs. [22] and [23], respectively. Until now, none of these ideas have direct experimental verification.

In this Letter, we propose another strongly interacting neutrino scenario to solve the GZK problem, which – in contrast to previous proposals – is based entirely on the Standard Model of particle physics. It exploits non-perturbative electroweak instanton-induced processes for the interaction of cosmogenic neutrinos with nucleons in the atmosphere, which may have a sizeable cross-section above a threshold energy $E_{\rm th} = \mathcal{O}((4\pi M_W/\alpha_W)^2)/(2m_p) = \mathcal{O}(10^{18})$ eV, where M_W denotes the

[1] There is an ongoing debate whether the excess of events above $E_{\rm GZK}$ is significant and whether the data from different collaborations are mutually consistent [8]. We will comment on this point below.

W-boson mass and α_W the electroweak fine structure constant [24, 25, 26]. For the first time in the literature, we present a detailed statistical analysis of the agreement between observations and predictions from strongly interacting neutrino scenarios.

Our scenario can be summarized as follows. We assume a standard power-like primary spectrum for protons injected from sources at cosmological distances, which extends beyond the GZK cutoff. After propagation through the CMB, the protons – arriving at earth mostly with energies below $E_{\rm GZK}$ – will be one component of the observed cosmic ray spectrum. The spectrum of the produced cosmogenic neutrinos is entirely determined by the proton injection spectrum and can therefore be determined precisely, including all known effects. The cosmogenic neutrinos travel unaffected through the CMB. However, for energies above $\approx 10^{19}$ eV, they have a large cross-section for interactions with nuclei in the atmosphere due to electroweak instanton-induced processes. They give rise, therefore, to a second, predictable component of the observed cosmic ray spectrum, which dominates above the GZK cutoff over the first, proton-initiated component. Our proposal leads to an explanation of the observed cosmic ray spectrum simultaneously above and below the GZK cutoff, without the need to fix the ratio of the fluxes below and above $E_{\rm GZK}$ by hand[2], as it is necessary in most alternative proposals. The goodness of the scenario is studied by statistical methods and an excellent agreement is seen between the predictions and the observations.

Our analysis proceeds in three steps, which are performed in Sects. 2, 3, and 4. *i)* First, we study the consequences of a power-like proton injection spectrum. We determine the resulting proton and neutrino fluxes on earth, taking into account the appropriate types of energy losses. *ii)* In the second step, we calculate the spectrum of cosmogenic neutrino-initiated electroweak instanton-induced air showers. *iii)* The third step consists in the comparison of the observed UHECR spectrum with the prediction arising from an inclusion of instanton-induced processes. Based on the goodness of the scenario, we determine the confidence region in the parameter space of our scenario. Finally, we summarize our result and present our conclusions in Sect. 5.

2 Proton and cosmogenic neutrino fluxes

We start with a power-like injection spectrum per co-moving volume of protons with energy E_i, spectral index α, and redshift (z) evolution index m,

$$j_p = j_0 \, E_i^{-\alpha} \, (1+z)^m \, \theta(E_{\rm max} - E_i) \, \theta(z - z_{\rm min}) \, \theta(z_{\rm max} - z) \, . \qquad (1)$$

Here, j_0 is a normalization factor, $E_{\rm max}$ is the maximal energy, which can be reached through astrophysical accelerating processes in a bottom-up scenario, and $z_{\rm min/max}$ take into account that nearby/very early there are no astrophysical sources. As we will see in our comparison with UHECR data in Sect. 4, the overall normalization j_0 is fixed by the observed flux, and our predictions are quite insensitive to the specific choice for $E_{\rm max}$, $z_{\rm min}$, and $z_{\rm max}$, within their anticipated values. The main sensitivity arises from the spectral parameters α and m, for which we determine the 1- and 2-sigma confidence regions in Sect. 4.

The injected protons propagate through the CMB. This propagation can be described [27] by $P_{b|a}(r, E_i; E)$ functions, which give the expected number of particles of type b above the threshold

[2] This feature is shared with all strongly interacting neutrino scenarios. In contrast to these other scenarios, in our case, however, the threshold energy is automatically fixed by Standard Model parameters (M_W and α_W).

energy E if one particle of type a started at a distance r with energy E_i. With the help of these propagation functions, the differential flux of protons ($b = p$) and cosmogenic neutrinos ($b = \nu_i, \bar{\nu}_i$) at earth, i.e. their number N_b arriving at earth with energy E per units of energy, area (A), time (t) and solid angle (Ω), can be expressed as

$$F_b(E) \equiv \frac{\mathrm{d}^4 N_b}{\mathrm{d}E\,\mathrm{d}A\,\mathrm{d}t\,\mathrm{d}\Omega} = \int_0^\infty \mathrm{d}E_i \int_0^\infty \mathrm{d}r\ (1+z(r))^3\ (-)\frac{\partial P_{b|p}(r, E_i; E)}{\partial E}\, j_p(r, E_i)\,. \qquad (2)$$

In our analysis we go, according to $\mathrm{d}z = -(1+z)\,H(z)\,\mathrm{d}r/c$, out to distances $R_{\max}$ corresponding to $z_{\max} = 2$ (cf. Ref. [28]), while we choose $z_{\min} = 0.012$ in order to take into account the fact that within 50 Mpc there are no astrophysical sources of UHECRs. We use the expression

$$H^2(z) = H_0^2\ \left[\Omega_M\,(1+z)^3 + \Omega_\Lambda\right] \qquad (3)$$

for the relation of the Hubble expansion rate at redshift z to the present one. Uncertainties of the latter, $H_0 = h$ 100 km/s/Mpc, with $h = (0.71 \pm 0.07)\times^{1.15}_{0.95}$ [29], are included. In Eq. (3), Ω_M and Ω_Λ, with $\Omega_M + \Omega_\Lambda = 1$, are the present matter and vacuum energy densities in terms of the critical density. As default values we choose $\Omega_M = 0.3$ and $\Omega_\Lambda = 0.7$, as favored today. Our results turn out to be pretty insensitive to the precise values of the cosmological parameters.

We calculated $P_{b|a}(r, E_i; E)$ in two steps. *i)* First, the SOPHIA Monte-Carlo program [30] was used for the simulation of photohadronic processes of protons with the CMB photons. For e^+e^- pair production we used the continuous energy loss approximation, since the inelasticity is very small ($\approx 10^{-3}$). We calculated the $P_{b|a}$ functions for "infinitesimal" steps ($1 \div 10$ kpc) as a function of the redshift z. *ii)* We multiplied the corresponding infinitesimal probabilities starting at a distance $r(z)$ down to earth with $z = 0$. The details of the calculation of the $P_{b|a}(r, E_i; E)$ functions for protons, neutrinos, charged leptons, and photons will be published elsewhere [31].

The determination of the propagation functions took approximately one day on an average personal computer. In this connection, the advantage of the formulation of the spectra (2) in terms of the propagation functions becomes evident. The latter have to be determined only once and for all. Without the use of the propagation functions, one would have to perform a simulation for any variation of the input spectrum ($\alpha, m, \ldots$), which requires excessive computer power. Since the propagation functions are of universal usage, we decided to make the latest versions of $-\partial P_{b|a}/\partial E$ available for the public via the World-Wide-Web URL www.desy.de/~uhecr .

As a check on our propagation functions, we have compared our predictions for the spectra (2) with the ones presented in Ref. [17] for some specific values of the spectral parameters (α, m, $E_{\max}$, $z_{\min}$, $z_{\max}$, j_0) and found quite good agreement.

3 Spectrum of instanton-induced air showers

In this section, we exploit a recent prediction of the electroweak instanton-induced parton-parton cross-section [26] and determine the spectrum of instanton-induced air showers, which are initiated by the cosmogenic neutrino flux (2) impinging on the earth's atmosphere.

Let us start with a review of the current knowledge about electroweak instantons. In the Standard Model of electroweak interactions (Quantum Flavor Dynamics (QFD)) there are certain processes which fundamentally can not be described by ordinary perturbation theory. These processes are

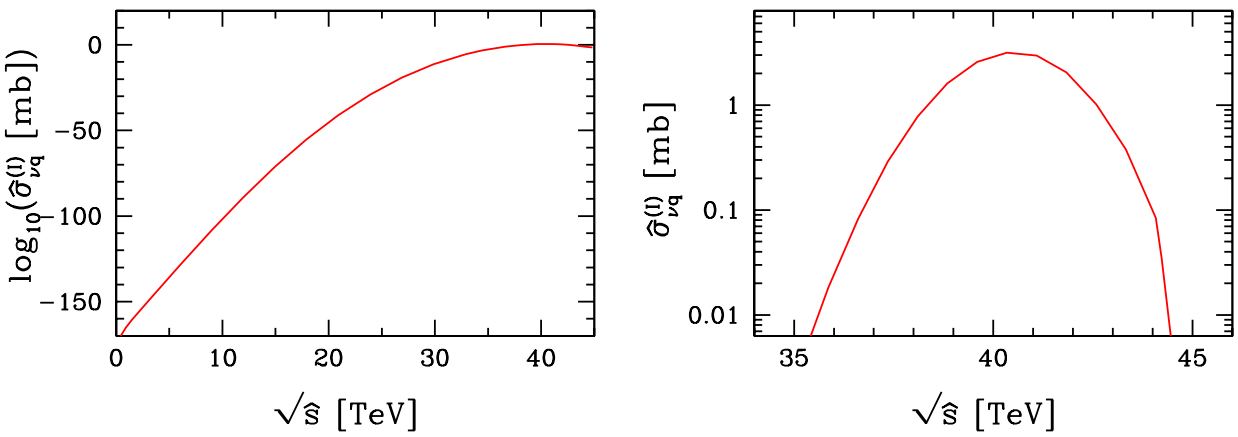

Figure 1: The electroweak instanton-induced neutrino-quark cross-section $\hat{\sigma}^{(I)}_{\nu q}$ as predicted in Ref. [26] for the whole range of the CM energy $\sqrt{\hat{s}}$ (left) and near the maximum (right).

associated with axial anomalies and manifest themselves as anomalous violation of baryon plus lepton number $(B + L)$ [32]. They are induced by topological fluctuations of the non-Abelian gauge fields, notably by instantons [33]. In Minkowski space-time, instantons describe tunneling transitions between degenerate, topologically inequivalent vacua. The corresponding tunneling barrier is given by the energy of the sphaleron [34], an unstable static solution of the Yang-Mills equations, and of order $M_{\rm sp} \approx \pi M_W/\alpha_W \approx 10$ TeV. The corresponding processes violate $B + L$ according to the selection rule $\triangle B = \triangle L = -3$.

It is generally accepted that such topological fluctuations and the associated $B + L$ violating processes are very important at high temperatures [35] and have therefore a crucial impact on the evolution of the baryon and lepton asymmetries of the universe[3]. It is, however, still debated whether manifestations of such fluctuations – involving notably the associated production of $\mathcal{O}(1/\alpha_W) \approx 30$ W/Z-bosons in addition to the anomalously produced quarks and leptons – may be directly observed in high-energy scattering processes [24]. Despite considerable theoretical [41] and phenomenological [25, 42] efforts, the actual size of the cross-sections in the relevant, tens of TeV energy regime was never unanimously established (for reviews, see Refs. [37, 43]).

There is a close analogy [44] between QFD and hard QCD instanton-induced processes in deep-inelastic scattering [45]. Recent information about the latter – both from lattice simulations [46] and from the H1 experiment at HERA [47] – has been used by one of the authors to learn about the fate of electroweak $B + L$ violation and associated multi-W/Z production at high energies [26] (for a review, see Ref. [48]). The prediction for the electroweak instanton-induced neutrino-quark cross-section $\hat{\sigma}^{(I)}_{\nu q}$ is displayed in Fig. 1 as a function of the neutrino-quark center-of-mass (CM) energy $\sqrt{\hat{s}}$. At small CM energies, the cross-section is really tiny, e.g. $\hat{\sigma}^{(I)}_{\nu q} \approx 10^{-141}$ pb at $\sqrt{\hat{s}} \approx 3$ TeV, but steeply growing. Nevertheless, it stays unobservably small, $\hat{\sigma}^{(I)}_{\nu q} \lesssim 10^{-26}$ pb for $\sqrt{\hat{s}} \lesssim 22.5$ TeV, in the quite conservative fiducial kinematical region inferred via the QFD–QCD analogy from lattice data and HERA. It was noted that a slight extrapolation towards larger energies – still compatible with lattice results and HERA – points to a cross-section $\approx 10^{-6}$ pb at a CM energy of about 30 TeV, which is within the reach of the Very Large Hadron Collider.

[3]Standard Model electroweak baryogenesis seems excluded, however, due to the weakness of the electroweak phase transition [36] (for reviews, see Refs. [37, 38]), while thermal leptogenesis [39, 40] is quite successful.

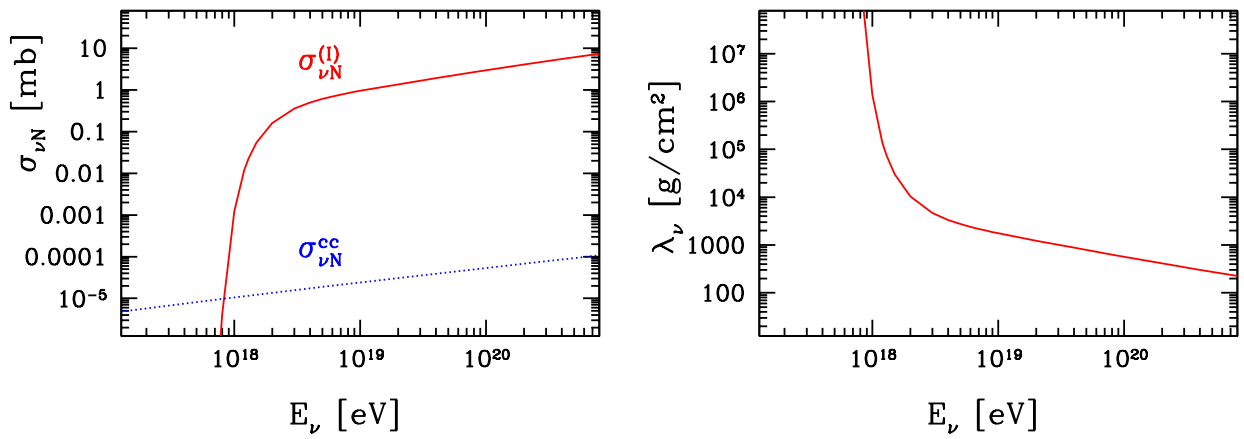

Figure 2: *Left:* Prediction of the electroweak instanton-induced neutrino-nucleon cross-section $\sigma^{(I)}_{\nu N}$ (solid) in comparison with the charged current cross-section $\sigma^{\rm cc}_{\nu N}$ (dotted) from Ref. [50], as a function of the neutrino energy E_ν in the nucleon's rest frame. *Right:* Neutrino interaction length due to combined effects of charged current interactions and instanton-induced processes.

In this Letter, we will use the prediction from Ref. [26] even at higher energies[4], up to and above $\sqrt{\hat{s}} \approx 40$ TeV, where the cross-section reaches its maximum of order a few millibarn (cf. Fig. 1 (right)). The corresponding neutrino-nucleon cross-section is obtained after folding the parton cross-section $\sigma^{(I)}_{\nu q}$ with the quark density functions f_q,

$$\sigma^{(I)}_{\nu N}(s) = \sum_q \int_0^1 {\rm d}x\, f_q(x,\mu)\, \hat{\sigma}^{(I)}_{\nu q}(xs)\,, \tag{4}$$

where s denotes the neutrino-nucleon CM energy squared and μ the factorization scale. For our numerical integration we have used various sets of parton distributions as they are implemented in the parton distribution library PDFLIB [49]. Uncertainties associated with different parton distribution sets are in the $\mathcal{O}(20)\,\%$ range and are not explicitely shown in the following. Figure 2 (left) displays the prediction of the electroweak instanton-induced neutrino-nucleon cross-section as a function of the neutrino energy E_ν in the nucleon's rest frame for a choice $\mu = M_W$ of the factorization scale. Above a threshold at about $E_\nu \approx 10^{18}$ eV, it quickly reaches one millibarn at about 10^{19} eV, and tends to grow power-like, due to the growth of the sea quark distributions in the nucleon at small x, quite analogous to the standard charged current cross-section $\sigma^{\rm cc}_{\nu N}$ (cf. Fig. 2 (left)). It should be noted that such a cross-section will lead, via dispersion relations, to lower energy deviations of Standard Model predictions for elastic scattering from their perturbative values [37]. However, it is easily checked that, for the one shown in Fig. 2 (left), these corrections will be unobservably small in the energy regime available at present accelerators [51].

The corresponding neutrino interaction length $\lambda_\nu \equiv m_p/\sigma^{\rm tot}_{\nu N}$, with $\sigma^{\rm tot}_{\nu N} = \sigma^{\rm cc}_{\nu N} + \sigma^{(I)}_{\nu N}$, is shown in Fig. 2 (right). It falls below $X_0 = 1031$ g/cm^2 – the vertical depth of the atmosphere at sea level[5] – for $E_\nu \gtrsim 3\cdot 10^{19}$ eV. The apparent success of our scenario is based on the unexpected coincidence of

[4] It should be kept in mind, however, that, at the energies of interest here, the prediction in Fig. 1 is rather an educated extrapolation or guess (cf. Ref. [26]).

[5] For our numerical calculations involving the atmospheric depth $X(\theta)$ we have used a parametrization of the US Standard Atmosphere (1976) from Ref. [52].

this scale and $E_{\rm GZK}$. Above this energy, the atmosphere becomes opaque to cosmogenic neutrinos and all of them will end up as air showers. Quantitatively, this fact can be described by

$$F^{(I)}(E) \equiv \frac{{\rm d}^4 N^{(I)}}{{\rm d}E\,{\rm d}t\,{\rm d}A\,{\rm d}\Omega} = \frac{\sigma^{(I)}_{\nu N}(E)}{\sigma^{\rm tot}_{\nu N}(E)}\,F_\nu(E)\,\left[1-{\rm e}^{-\frac{X(\theta)}{\lambda_\nu(E)}}\right]\,, \tag{5}$$

which gives the spectrum of neutrino-initiated instanton-induced air showers, for an incident cosmogenic neutrino flux $F_\nu = \sum_i [F_{\nu_i} + F_{\bar\nu_i}]$ from Eq. (2), in terms of the atmospheric depth[5] $X(\theta)$, with θ being the zenith angle. For $E_\nu \gtrsim 3\cdot 10^{19}$ eV, one has $\lambda_\nu(E_\nu) < X_0$, and the spectrum (5) quickly equals the incident cosmogenic neutrino flux, $F_\nu(E)$. For $E_\nu \lesssim 4\cdot 10^{18}$ eV, on the other hand, the cross-section $\sigma^{\rm tot}_{\nu N}(E_\nu) \lesssim 0.56$ mb corresponds to a neutrino interaction length $\lambda_\nu(E_\nu) \gtrsim 3000$ g/cm^2, which is comparable to the atmospheric depth at larger zenith angles, $\theta \gtrsim 70^\circ$. Therefore, for these energies, neutrino-initiated electroweak instanton-induced showers can be searched for at cosmic ray facilities by looking for quasi-horizontal air showers, $\theta \gtrsim 70^\circ$ [25]. At the end of Sect. 4, we will show that the rate from our prediction (5) is consistent with observational constraints found by the Fly's Eye [53] and AGASA [54] collaborations.

Equation (5) does not account for the efficiency of an air shower array to trigger on low altitude air showers. Below 10^{19} eV, neutrino-induced showers may be initiated so close to the array that the showers do not spread out sufficiently to trigger the array. As discussed in Ref. [25], one may suppose that an array does not trigger on showers initiated within $X_{\rm tr} = 500$ g/cm^2 of the detection level. This can be implemented in Eq. (5) by replacing $X(\theta)$ with $(X(\theta) - X_{\rm tr})$. Such an assumption seems reasonable for vertical showers seen by a ground array (AGASA), but is somewhat pessimistic for showers at larger zenith angles or for fluorescence detectors (HiRes). We have performed our fit in Sect. 4 with/without such a "trigger" cut for AGASA/HiRes data. Its effect, however, turned out to be negligible.

Proton-initiated electroweak instanton-induced air showers have been quite intensively studied in Ref. [25] and compared to generic proton- or iron-initiated air showers[6]. While identifiable systematic differences between average showers of different origin could be found, the differences did not appear to be sufficient to discriminate between proton-initiated instanton-induced showers and fluctuations in generic showers. The same is expected for neutrino-initiated instanton-induced air showers, as long as the first interaction occurs sufficiently high in the atmosphere, at a depth $\lesssim 500$ g/cm^2, which happens in our case for $E_\nu \gtrsim 10^{20}$ eV. We will find from our fits in the next section that the contribution of cosmogenic neutrino-initiated air showers to the UHECR spectrum starts to dominate at around this energy over the proton-initiated generic component.

4 Comparison with UHECR data

In this section, we compare the predicted air shower spectrum from Eqs. (2) and (5), the latter averaged over the appropriate range of zenith angles θ,

$$F_{\rm pred}(E;\alpha,m,E_{\rm max},z_{\rm min},z_{\rm max},j_0) = F_p(E;\ldots) + F^{(I)}(E;\ldots)\,, \tag{6}$$

[6] On account of $\sigma^{(I)}_{pN} \ll \sigma^{\rm gen}_{pN} \approx 100$ mb, where $\sigma^{\rm gen}_{pN}$ is the cross-section for generic proton-nucleon processes, the contribution of proton-initiated instanton-induced air showers to the UHECR spectrum can be safely ignored.

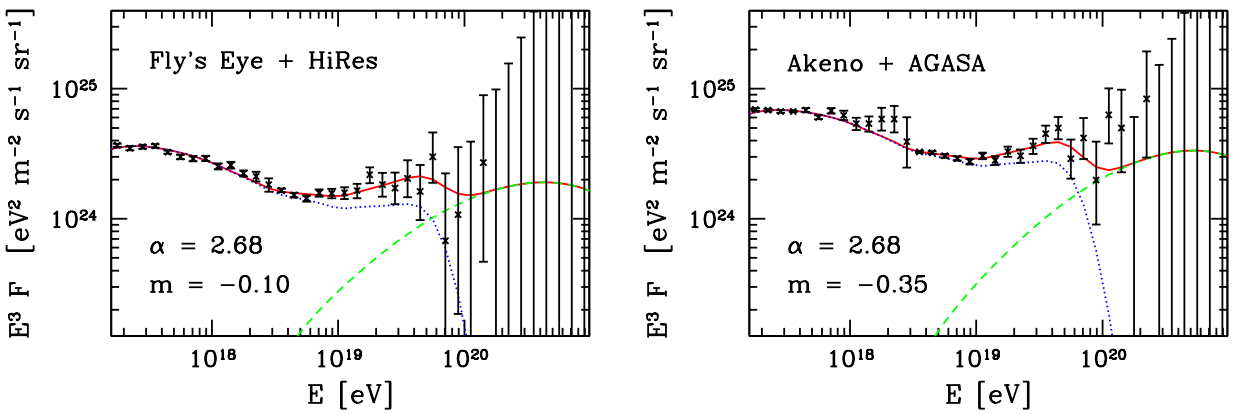

Figure 3: Ultrahigh energy cosmic ray data (points with statistical error bars; *left:* combination of Fly's Eye and HiRes data; *right:* combination of Akeno and AGASA data) and their best fits within the electroweak instanton scenario (solid) for $E_{\max} = 3 \cdot 10^{22}$ eV, $z_{\min} = 0.012$, $z_{\max} = 2$, consisting of a proton component (dotted) plus a cosmogenic neutrino-initiated electroweak instanton-induced component (dashed).

with the observations. We perform a detailed statistical analysis and present a measure for the goodness of the instanton-induced scenario.

The analysis consists of two parts. *i)* The UHECR collaborations give their results for the incoming flux in a binned form. Note, however, that the number of events in a given bin is integer and follows the Poisson distribution. In order to be able to give the goodness of the instanton-induced scenario by statistical methods, we determine the number of experimentally observed events in a given energy bin by converting the published values of the cosmic ray flux. We analyse the results from different experimental settings separately and perform the UHECR analysis for the two most recent results from the HiRes and AGASA collaborations, respectively. *ii)* We determine the 1-sigma and 2-sigma confidence regions for the parameters (α, m) characterizing the proton injection spectrum (cf. Sect. 2). The method is similar to the frequentist's analysis [29] and uses a Monte-Carlo integration in the multi-dimensional space of bins.

ad i) In our comparison, we use the observed data from $\log(E/\text{eV}) = 17.2$ to $\log(E/\text{eV}) = 21$. We have altogether 38 bins. The bins with the largest energies are empty. This non-trivial information is incorporated into the analysis, too. In the low energy region, there are no published results available from AGASA and only low statistics results from HiRes-2. Therefore, we included the results of the predecessor collaborations – Akeno [55] and Fly's Eye, respectively – into the analysis. With a small normalization correction, it was possible to continuously connect the AGASA data [1] with the Akeno ones and the HiRes-1 monocular data [4] with the Fly's Eye stereo ones [2], respectively (cf. Fig. 3). Usually, it is advisable to avoid the combination of different experimental data. Since in the present case it is interesting to see how well our scenario works for energies below and above the GZK cutoff, we used the less problematic solution and combined results from experiments with the same techniques and with largely overlapping experimental groups. The normalization was matched at $\log(E/\text{eV}) = 18.5$ for both cases.

Note that the highest energy event of HiRes was published using a five times bigger bin size than for other energies [4]. In order to preserve information, we prefer to keep the binning, give the particular bin with one event, and present upper bounds for the bins with zero event. From the

published data of HiRes, we determined the approximate energy and the corresponding bin of the highest energy event.

ad ii) The goodness of the scenario is determined by a statistical analysis. In order to give the confidence region in the α–m plane, we determined the compatibility of different (α, m) pairs with the experimental data. For some fixed (α,m) pair, one can determine the expected number of event in individual bins ($\lambda = \{\lambda_1, ..., \lambda_r\}$, where the λ_i-s are non-negative, usually non-integer numbers and in our case the number of variables corresponds to the number of bins, thus r=38). For this specific (α, m), the probability distribution in the i-th bin is given by the Poisson distribution with mean λ_i. The r dimensional probability distribution $P(\mathbf{k})$ is just the product of the individual Poisson distributions (here $\mathbf{k} = \{k_1, ...k_r\}$ is a set of non-negative integer numbers). It is easy to include also the $\approx 30\%$ overall uncertainty in the energy measurement of the experiments into the $P(\mathbf{k})$ probability. We denote the experimental result by $\mathbf{n} = \{n_1, ...n_r\}$, where the n_i-s are non-negative, integer numbers. According to the r dimensional probability distribution, the experimentally observed event set $\mathbf{n}$ has a definite, though usually very small probability $P(\mathbf{n})$. The (α, m) pair is compatible with the experimental results if

$$\sum_{\mathbf{k}|P(\mathbf{k})>P(\mathbf{n})} P(\mathbf{k}) < s\,. \tag{7}$$

For a 1-(or 2-)sigma compatibility one takes s=0.68 (or s=0.95), respectively. The best fit is found by minimizing the sum on the left hand side. This technique is equivalent with the χ^2 technique for a large class of problems[7]. Note, however, that the χ^2 technique always gives a confidence region and the χ^2/d.o.f is used as an estimate for the goodness of the scenario. Since χ^2/d.o.f can be directly interpreted for Gaussian problems only, our goodness of the scenario technique is more general.

Since we have 38 variables, it is practically impossible to calculate the sum in equation (7) exactly. Fortunately, there is no need for the exact calculation, the sum can be determined with arbitrary precision by using an importance sampling based Monte-Carlo summation. Since the sum of the individual probabilities is one, the left-hand-side of equation (7) can be rewritten as

$$\sum_{\mathbf{k}|P(\mathbf{k})>P(\mathbf{n})} P(\mathbf{k}) = \frac{\sum_{\mathbf{k}} P(\mathbf{q})\,\theta[P(\mathbf{k}) - P(\mathbf{p})]}{\sum_{\mathbf{k}} P(\mathbf{k})}\,. \tag{8}$$

Equation (8) defines the Monte-Carlo summation straightforwardly. When calculating the sum, numbers with Poisson distribution are generated for $\mathbf{k}$ and only those are taken in the sum, for which $P(\mathbf{k}) > P(\mathbf{p})$.

Figure 3 shows our best fits for the HiRes and for the AGASA UHECR data (the lower energy data is also included, as we explained before). The best fit values are $\alpha = 2.68$, $m = -0.1$, for HiRes, and $\alpha = 2.68$, $m = -0.35$, for AGASA. We can see very nice agreement with the data within an energy range of nearly four orders of magnitude. The fits are insensitive to the value of $E_{\max}$ as far as we choose a value above $\approx 3 \cdot 10^{21}$ eV. The shape of the curve between 10^{17} eV and 10^{19} eV is mainly determined by the redshift evolution index m. At $z = 0$, below 10^{18} eV the attenuation length of protons is already around the size of the universe. Therefore, one would expect no distortions of the injected spectrum below this energy and an accumulation of particles

[7]For the application of the χ^2 technique with UHECR data, see Refs. [11, 56].

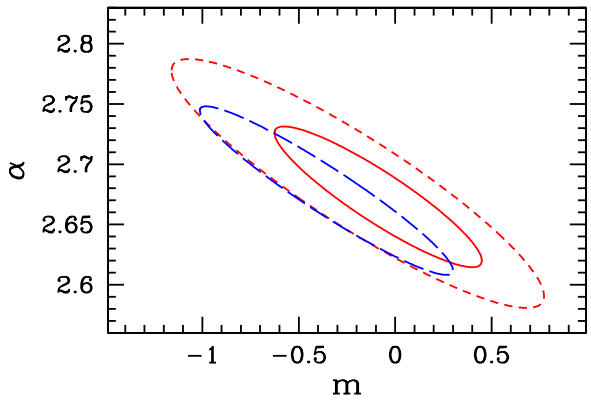

Figure 4: Confidence regions in the power-law index α and the redshift evolution index m of the primary proton injection spectrum, for fits to the Fly's Eye + HiRes data (1-sigma (solid); 2-sigma (short-dashed)) and to Akeno + AGASA data (2-sigma (long dashed)), respectively, for $E_{\rm max} \gtrsim 3 \cdot 10^{21}$ eV, $z_{\rm min} \geq 0$, $z_{\rm max} = 2$.

just above it. However, at larger redshifts, the interaction lengths are smaller and the spectrum of particles created at cosmological distances has an accumulation peak at lower energies. The more particles are created at large distances (i.e. the larger m is), the stronger this effect will be[8]. The peak around $4 \cdot 10^{19}$ eV shows the accumulation of particles due to the GZK effect. Neutrinos start to dominate over protons at around 10^{20} eV.

It is important to note that, if we omit the neutrino component, then the model is ruled out on the 3-sigma level for both experiments. This is due to the fact that there are no nearby sources ($z_{\rm min} \neq 0$) and all the events above 10^{20} eV are highly inconsistent with the predictions. A choice of $z_{\rm min} = 0$ makes the HiRes data compatible with a proton-only scenario on the 2-sigma level (see also Refs. [4, 8]). If neutrinos are included, then – as they dominate over protons above 10^{20} eV – the fit results cease to be sensitive to the value of $z_{\rm min}$.

Figure 4 displays the confidence regions in the $\alpha - m$ plane for HiRes and AGASA. The scenario is consistent on the 2-sigma level with both experiments. For HiRes, the compatibility is even true on the 1-sigma level. It is important to note that both experiments favor the same values for α and m, demonstrating their mutual compatibility on the 2-sigma level. If we ignore the energy uncertainty in the determination of the goodness of the fit, they turn out to be inconsistent.

Finally, let us discuss the consistency of our scenario with the currently available limits on deeply penetrating showers from Fly's Eye [53] and AGASA [54]. Taking into account – in distinction to Ref. [57] – the atmospheric attenuation of the cosmogenic neutrino flux predicted in our scenario and the uncertainties in the estimate of the range of depth within which the shower must originate to trigger the array, we find that AGASA should have seen $1 \div 10$ quasi-horizontal air showers ($\theta \gtrsim 60^\circ$) from the electroweak instanton-induced processes during a running time of 1710.5 days. This is consistent with AGASA's present analysis of their respective data [54]. The Fly's Eye upper limit on the product of the total neutrino flux times neutrino-nucleon cross-section, $(F_\nu \, \sigma_{\nu N}^{\rm tot})_{\rm Fly's\ Eye}$ [53], in the energy range $10^{17 \div 20}$ eV, can be translated, for a given

[8] Our finding suggests that the extragalactic UHECR component begins to dominate over the galactic one already at $\approx 10^{17}$ eV. If we start our fit at $10^{18.5}$ eV – assuming that the galactic component dominates up to this energy – we find a very mild dependence on m and the same best fit values for α, with a bit larger uncertainties.

predicted neutrino flux $F_\nu^{\rm pred}$, into an upper limit on $\sigma_{\nu N}^{\rm tot} < (F_\nu\, \sigma_{\nu N}^{\rm tot})_{\rm Fly's\ Eye}/F_\nu^{\rm pred}$, as long as it is smaller than 10 μb [25, 58]. We find that, for our predicted cosmogenic neutrino flux, the right-hand-side of this inequality is larger than 10 μb in the whole energy range, such that the Fly's Eye non-observation of quasi-horizontal air showers does not give any constraint. We therefore conclude that our prediction of the neutrino-nucleon cross-section, as shown in Fig. 2 (left), does not contradict any constraints from cosmic ray experiments so far, as long as the ultrahigh energy cosmic neutrino flux is at the cosmogenic level we have predicted.

5 Summary and conclusions

We have shown that a simple scenario with a single power-like injection spectrum of protons can describe all the features of the UHECR spectrum in the energy range $10^{17\div21}$ eV. In this scenario, the injected protons produce neutrinos during their propagation by interacting with the CMB. Through Standard Model electroweak instanton-induced processes, these neutrinos may interact with the atmosphere and give rise to a non-negligible contribution to the detected air showers at the highest energies. The model has few parameters from which only two – the power index α and the redshift evolution index m – has a strong effect on the final shape of the spectrum. We found that for certain values of α and m this scenario is compatible with the available observational data from the HiRes and AGASA experiments (combined with their predecessor experiments, Fly's Eye and Akeno, respectively) on the 2-sigma level (also 1-sigma for HiRes). The ultrahigh energy neutrino component can be experimentally tested by studying the zenith angle dependence of the events in the range $10^{18\div20}$ eV at cosmic ray facilities such as the Pierre Auger Observatory and by looking for spatially compact energetic μ bundles at neutrino telescopes such as AMANDA [25].

Finally, let us emphasize that the same fit results are valid for all strongly interacting neutrino models if the neutrino-nucleon cross-section has a similar threshold-like behaviour as in Fig. 2. The instanton scenario, however, has the advantage that it is based solely on the Standard Model and can be falsified in the near future by a negative outcome of QCD instanton searches at HERA.

Acknowledgements

We thank D. V. Semikoz for useful discussions about the cosmogenic neutrino flux. This work was partially supported by Hungarian Science Foundation grants No. OTKA-T034980/T037615.

References

[1] M. Takeda *et al.*, Phys. Rev. Lett. **81** (1998) 1163;
http://www-akeno.icrr.u-tokyo.ac.jp/AGASA/ ; date: 24$^{\rm th}$ February 2003.

[2] D. J. Bird *et al.*, Phys. Rev. Lett. **71** (1993) 3401; Astrophys. J. **424** (1994) 491; *ibid.* **441** (1995) 144.

[3] M. A. Lawrence, R. J. Reid and A. A. Watson, J. Phys. G **17** (1991) 733; M. Ave, J. A. Hinton, R. A. Vazquez, A. A. Watson and E. Zas, Phys. Rev. Lett. **85** (2000) 2244.

[4] T. Abu-Zayyad *et al.* [HiRes Collaboration], astro-ph/0208243; astro-ph/0208301.

[5] N.N. Efimov *et al.*, in *Proc. of the Astrophysical Aspects of the Most Energetic Cosmic Rays* (World Scientific, Singapore, 1991).

[6] M. Nagano and A. A. Watson, Rev. Mod. Phys. **72** (2000) 689; L. Anchordoqui, T. Paul, S. Reucroft and J. Swain, hep-ph/0206072.

[7] K. Greisen, Phys. Rev. Lett. **16** (1966) 748; G. T. Zatsepin and V. A. Kuzmin, JETP Lett. **4** (1966) 78 [Pisma Zh. Eksp. Teor. Fiz. **4** (1966) 114].

[8] J. N. Bahcall and E. Waxman, Phys. Lett. B **556** (2003) 1; D. De Marco, P. Blasi and A. V. Olinto, astro-ph/0301497.

[9] V. S. Beresinsky and G. T. Zatsepin, Phys. Lett. B **28** (1969) 423.

[10] D. Fargion, B. Mele and A. Salis, Astrophys. J. **517** (1999) 725; T. J. Weiler, Astropart. Phys. **11** (1999) 303; S. Yoshida, G. Sigl and S. j. Lee, Phys. Rev. Lett. **81** (1998) 5505.

[11] Z. Fodor, S. D. Katz and A. Ringwald, Phys. Rev. Lett. **88** (2002) 171101; JHEP **0206** (2002) 046.

[12] O. E. Kalashev, V. A. Kuzmin, D. V. Semikoz and G. Sigl, Phys. Rev. D **65** (2002) 103003.

[13] E. Andres *et al.* [AMANDA Collaboration], Nature **410** (2001) 441.

[14] I. Kravchenko *et al.* [RICE Collaboration], astro-ph/0112372.

[15] D. Zavrtanik [AUGER Collaboration], Nucl. Phys. Proc. Suppl. **85** (2000) 324.

[16] S. Yoshida and M. Teshima, Prog. Theor. Phys. **89** (1993) 833; R. J. Protheroe and P. A. Johnson, Astropart. Phys. **4** (1996) 253; S. Yoshida, H. y. Dai, C. C. Jui and P. Sommers, Astrophys. J. **479** (1997) 547; R. Engel and T. Stanev, Phys. Rev. D **64** (2001) 093010.

[17] O. E. Kalashev, V. A. Kuzmin, D. V. Semikoz and G. Sigl, Phys. Rev. D **66** (2002) 063004.

[18] J. Bordes *et al.*, hep-ph/9705463; Astropart. Phys. **8** (1998) 135.

[19] G. Domokos, S. Kovesi-Domokos and P. T. Mikulski, hep-ph/0006328.

[20] G. Domokos and S. Kovesi-Domokos, Phys. Rev. Lett. **82** (1999) 1366; S. Nussinov and R. Shrock, Phys. Rev. D **59** (1999) 105002; P. Jain, D. W. McKay, S. Panda and J. P. Ralston, Phys. Lett. B **484** (2000) 267.

[21] M. Kachelriess and M. Plümacher, Phys. Rev. D **62** (2000) 103006; L. Anchordoqui, H. Goldberg, T. McCauley, T. Paul, S. Reucroft and J. Swain, Phys. Rev. D **63** (2001) 124009.

[22] G. Domokos and S. Nussinov, Phys. Lett. B **187** (1987) 372.

[23] S. Barshay and G. Kreyerhoff, Eur. Phys. J. C **23** (2002) 191; Phys. Lett. B **535** (2002) 201; L. A. Anchordoqui, J. L. Feng and H. Goldberg, Phys. Lett. B **535** (2002) 302;

[24] H. Aoyama and H. Goldberg, Phys. Lett. B **188** (1987) 506; A. Ringwald, Nucl. Phys. B **330** (1990) 1; O. Espinosa, Nucl. Phys. B **343** (1990) 310; V. V. Khoze and A. Ringwald, Phys. Lett. B **259** (1991) 106.

[25] D. A. Morris and A. Ringwald, Astropart. Phys. **2** (1994) 43.

[26] A. Ringwald, Phys. Lett. B **555** (2003) 227.

[27] J. N. Bahcall and E. Waxman, Astrophys. J. **542** (2000) 543; Z. Fodor and S. D. Katz, Phys. Rev. D **63** (2001) 023002.

[28] E. Waxman, Astrophys. J. **452** (1995) L1.

[29] K. Hagiwara *et al.* [Particle Data Group Collaboration], Phys. Rev. D **66** (2002) 010001.

[30] A. Mücke *et al.*, Comput. Phys. Commun. **124** (2000) 290.

[31] Z. Fodor, S. D. Katz and A. Ringwald, in preparation.

[32] G. 't Hooft, Phys. Rev. Lett. **37** (1976) 8; Phys. Rev. D **14** (1976) 3432.

[33] A. A. Belavin *et al.*, Phys. Lett. B **59** (1975) 85; I. Affleck, Nucl. Phys. B **191** (1981) 429.

[34] F. R. Klinkhamer and N. S. Manton, Phys. Rev. D **30** (1984) 2212.

[35] V. A. Kuzmin, V. A. Rubakov and M. E. Shaposhnikov, Phys. Lett. B **155** (1985) 36; P. Arnold and L. D. McLerran, Phys. Rev. D **36** (1987) 581; A. Ringwald, Phys. Lett. B **201** (1988) 510.

[36] P. Arnold and O. Espinosa, Phys. Rev. D **47** (1993) 3546; Z. Fodor and A. Hebecker, Nucl. Phys. B **432** (1994) 127; K. Farakos, K. Kajantie, K. Rummukainen and M. E. Shaposhnikov, Nucl. Phys. B **425** (1994) 67; W. Buchmüller, Z. Fodor and A. Hebecker, Nucl. Phys. B **447** (1995) 317; F. Csikor, Z. Fodor and J. Heitger, Phys. Rev. Lett. **82** (1999) 21.

[37] V. A. Rubakov and M. E. Shaposhnikov, Usp. Fiz. Nauk **166** (1996) 493.

[38] M. Laine, in Proc. *International Workshop on Strong and Electroweak Matter (SEWM 2000)*, Marseille, France, 2000, hep-ph/0010275; W. Bernreuther, Lect. Notes Phys. **591** (2002) 237.

[39] M. Fukugita and T. Yanagida, Phys. Lett. B **174** (1986) 45.

[40] W. Buchmüller, in Proc. *European School of High-Energy Physics (ESHEP 2001)*, Beatenberg, Switzerland, 2001, hep-ph/0204288.

[41] L. D. McLerran, A. I. Vainshtein and M. B. Voloshin, Phys. Rev. D **42** (1990) 171; J. M. Cornwall, Phys. Lett. B **243** (1990) 271; P. B. Arnold and M. P. Mattis, Phys. Rev. D **42** (1990) 1738; S. Y. Khlebnikov, V. A. Rubakov and P. G. Tinyakov, Nucl. Phys. B **350** (1991) 441; A. H. Mueller, Nucl. Phys. B **348** (1991) 310; *ibid.* B **353** (1991) 44; V. V. Khoze and A. Ringwald, Nucl. Phys. B **355** (1991) 351.

[42] G. R. Farrar and R.-b. Meng, Phys. Rev. Lett. **65** (1990) 3377; A. Ringwald, F. Schrempp and C. Wetterich, Nucl. Phys. B **365** (1991) 3; M. J. Gibbs, A. Ringwald, B. R. Webber and J. T. Zadrozny, Z. Phys. C **66** (1995) 285.

[43] M. P. Mattis, Phys. Rept. **214** (1992) 159; P. G. Tinyakov, Int. J. Mod. Phys. A **8** (1993) 1823; R. Guida, K. Konishi and N. Magnoli, Int. J. Mod. Phys. A **9** (1994) 795.

[44] I. I. Balitsky and V. M. Braun, Phys. Lett. B **314** (1993) 237; A. Ringwald and F. Schrempp, in *Quarks '94*, Vladimir, Russia, 1994, hep-ph/9411217.

[45] S. Moch, A. Ringwald and F. Schrempp, Nucl. Phys. B **507** (1997) 134; A. Ringwald and F. Schrempp, Phys. Lett. B **438** (1998) 217; Comput. Phys. Commun. **132** (2000) 267; Phys. Lett. B **503** (2001) 331.

[46] D. A. Smith and M. J. Teper [UKQCD collaboration], Phys. Rev. D **58** (1998) 014505; A. Ringwald and F. Schrempp, Phys. Lett. B **459** (1999) 249.

[47] C. Adloff *et al.* [H1 Collaboration], Eur. Phys. J. C **25** (2002) 495.

[48] A. Ringwald, to appear in Proc. *26th Johns Hopkins Workshop on High-Energy Reactions*, Heidelberg, Germany, 2002, hep-ph/0302112.

[49] H. Plothow-Besch, Comput. Phys. Commun. **75** (1993) 396; Int. J. Mod. Phys. A **10** (1995) 2901; http://consult.cern.ch/writeups/pdflib/main.ps

[50] R. Gandhi, C. Quigg, M. H. Reno and I. Sarcevic, Phys. Rev. D **58** (1998) 093009.

[51] H. Goldberg and T. J. Weiler, Phys. Rev. D **59** (1999) 113005.

[52] R. Gandhi, C. Quigg, M. H. Reno and I. Sarcevic, Astropart. Phys. **5** (1996) 81.

[53] R. M. Baltrusaitis *et al.*, Phys. Rev. D **31** (1985) 2192.

[54] S. Yoshida *et al.* [AGASA Collaboration], in *Proc. 27th International Cosmic Ray Conference*, Hamburg, Germany, 2001, Vol. 3, p. 1142.

[55] M. Nagano *et al.*, J. Phys. G **18** (1992) 423.

[56] Z. Fodor and S. D. Katz, Phys. Rev. Lett. **86** (2001) 3224.

[57] L. A. Anchordoqui *et al.*, Phys. Rev. D **66** (2002) 103002.

[58] C. Tyler, A. V. Olinto and G. Sigl, Phys. Rev. D **63** (2001) 055001; A. Ringwald and H. Tu, Phys. Lett. B **525** (2002) 135.